# Neutron star structure with modern nucleonic three-body forces

Z. H. Li (李增花)[1] and H.-J. Schulze[2]
[1]*INFN-LNS, Via Santa Sofia 62, I-95123 Catania, Italy*
[2]*INFN Sezione di Catania, Via Santa Sofia 64, I-95123 Catania, Italy*
(Received 30 April 2008; revised manuscript received 26 June 2008; published 1 August 2008)

We provide convenient parametrizations of the high-density nuclear equation of state obtained within the Brueckner-Hartree-Fock approach using different modern nucleon-nucleon potentials together with compatible microscopic nuclear three-body forces. The corresponding neutron star mass-radius relations are also presented.

DOI: 10.1103/PhysRevC.78.028801 PACS number(s): 26.60.Kp, 21.45.Ff, 21.65.Mn, 24.10.Cn

*Introduction*. The theoretical investigation of dense stellar objects like neutron stars and supernovae requires the knowledge of the nucleonic equation of state (EOS) up to densities of about ten times normal nuclear density $\rho_0 = 0.17$ fm$^{-3}$. At these densities nucleonic three-body forces (TBF) contribute an important or even dominant part to the effective in-medium nucleon-nucleon interaction that is used within the different theoretical approaches like Brueckner-Hartree-Fock (BHF) [1], Dirac-BHF [2,3], variational [4,5], or Monte Carlo [6,7] method.

Consequently for reliable predictions theoretically well-controlled and consistent TBF are required. At present the theoretical status of microscopically derived TBF is still quite rudimentary: In most approaches semi-phenomenological TBF are used that involve several free parameters which are just fitted to the relevant data [4–8]. An important theoretical constraint is the consistency with a given two-body force, i.e., both two-body and three-body forces should be based on the same theoretical footing and use the same microscopical parameters in their construction.

We present in this report new results obtained within this framework, namely using meson-exchange TBF that employ the same meson-exchange parameters as an underlying nucleon-nucleon potential. In particular we show results based on the Argonne $V_{18}$ (V18) [9], the Bonn B (BOB) [10], and the Nijmegen 93 (N93) [11] potentials. For completeness we compare with results obtained with the widely used phenomenological Urbana-type (UIX) TBF [6,8] (in combination with the $V_{18}$ potential).

Our theoretical approach for calculating the EOS based on these interactions is the BHF formalism, for which the inclusion of TBF has been shown to be the dominant missing many-body effect [12–14], while three-hole line corrections are known to be small [15].

This Brief Report is based on Ref. [14], where detailed information on the construction of the microscopic TBF is given, and extends Ref. [16], where previous results obtained with the $V_{18}$ were presented. We begin with a short overview of the necessary formalism.

*Formalism*. At the present state of the art of the BHF approach, in order to avoid the very difficult problem of solving the relevant Faddeev equations as for the three-hole-line corrections, the TBF is reduced to an effective, density-dependent, two-body force by averaging over the third nucleon in the medium, the average being weighted by the BHF defect function $g$, which takes account of the nucleon-nucleon in-medium correlations [12,16–19]:

$$\overline{V}_{12}(\boldsymbol{r}) = \rho \int d^3 r_3 \sum_{\sigma_3,\tau_3} g(r_{13})^2 g(r_{23})^2 V_{123}\,. \tag{1}$$

The result is an effective two-nucleon potential with the operator structure

$$\begin{aligned}\overline{V}_{12}(\boldsymbol{r}) = {} & (\boldsymbol{\tau}_1\cdot\boldsymbol{\tau}_2)(\boldsymbol{\sigma}_1\cdot\boldsymbol{\sigma}_2)V_C(r) + (\boldsymbol{\sigma}_1\cdot\boldsymbol{\sigma}_2)V_S(r) + V_I(r) \\ & + S_{12}(\hat{\boldsymbol{r}})[(\boldsymbol{\tau}_1\cdot\boldsymbol{\tau}_2)V_T(r) + V_Q(r)],\end{aligned} \tag{2}$$

where $S_{12}(\hat{\boldsymbol{r}}) = 3(\boldsymbol{\sigma}_1\cdot\hat{\boldsymbol{r}})(\boldsymbol{\sigma}_2\cdot\hat{\boldsymbol{r}}) - \boldsymbol{\sigma}_1\cdot\boldsymbol{\sigma}_2$ is the tensor operator and the five components $V_O$, $O = C, S, I, T, Q$ depend on the nucleon density $\rho = \left(k_F^{(n)^3} + k_F^{(p)^3}\right)/3\pi^2$. They are added to the bare potential in the Bethe-Goldstone equation for the $G$ matrix,

$$G[E;\rho] = V + \sum_{k_a,k_b>k_F} V \frac{|k_a k_b\rangle\langle k_a k_b|}{E - e(k_a) - e(k_b) + i\varepsilon} G[E;\rho] \tag{3}$$

with $V = V_2 + V_3$, and are recalculated together with the defect function in every BHF iteration step until convergence is reached.

In the BHF approximation the energy per nucleon is then given by

$$\frac{B}{A} = \frac{3}{5}\frac{k_F^2}{2m} + \frac{1}{2\rho}\mathrm{Re}\sum_{k,k'\leqslant k_F}\langle kk'|G[e(k)+e(k');\rho]|kk'\rangle_a \tag{4}$$

and we present later the results obtained for symmetric nuclear matter and pure neutron matter. Furthermore, the well-tested [3,20–22] quadratic dependence on the proton fraction $x = \rho_p/\rho$,

$$\frac{B}{A}(\rho,x) = \frac{B}{A}(\rho,0.5) + (1-2x)^2 E_{\mathrm{sym}}(\rho), \tag{5}$$

where $E_{\mathrm{sym}}(\rho) = B/A(\rho,0) - B/A(\rho,0.5)$, is assumed in the calculation of beta-stable matter relevant for the determination of the neutron star mass-radius relations. The latter are obtained by solving the Tolman-Oppenheimer-Volkov equations in the standard manner [20,23,24].

 

TABLE I. Parameters of the EOS fit, Eq. (7), for symmetric nuclear matter and pure neutron matter and saturation properties of nuclear matter using different interactions.

| | Symmetric matter | | | Neutron matter | | | $[\rho, B/A]_0$ (fm$^{-3}$, MeV) | $K$ (MeV) | $E_{\rm sym}$ (MeV) | $E'_{\rm sym}$ (MeV) |
|---|---|---|---|---|---|---|---|---|---|---|
| | $\alpha$ | $\beta$ | $\gamma$ | $\alpha$ | $\beta$ | $\gamma$ | | | | |
| UIX | −452.5 | 556.0 | 1.24 | 78.0 | 232.9 | 2.24 | [0.18, −15.3] | 192 | 33.5 | 24.5 |
| V18 | −123.2 | 407.9 | 2.38 | 55.9 | 532.3 | 2.68 | [0.20, −14.7] | 226 | 30.6 | 33.8 |
| BOB | −130.4 | 537.0 | 2.39 | 31.0 | 780.2 | 2.77 | [0.17, −15.9] | 244 | 29.4 | 24.8 |
| N93 | −152.5 | 343.3 | 1.94 | 72.3 | 693.6 | 2.67 | [0.18, −15.4] | 216 | 34.0 | 35.5 |

The different meson-exchange contributions to the five components of the microscopic TBF, Eq. (2), are specified in detail in Ref. [14]. For the UIX TBF only the components $C, T, I$ are nonzero and are given explicitly by

$$\begin{aligned} V_O^{\rm UIX}(r_{12}) &= \rho \int d^3r_3\, g_x^2\, g_y^2 \\ &\times 4A\left[Y_x^\pi Y_y^\pi + 2P_r T_x^\pi T_y^\pi\right], \quad (O = C) \\ &\times 4A\left[P_x Y_x^\pi T_y^\pi + P_y Y_y^\pi T_x^\pi + P T_x^\pi T_y^\pi\right], \quad (O = T) \\ &\times 3U\left[\left(T_x^\pi T_y^\pi\right)^2\right], \quad (O = I) \end{aligned} \tag{6}$$

in the notation of Ref. [14]. Thus the $C$ and $T$ components correspond to the $\pi\pi$-$N\Delta$ part of the more general microscopic model, whereas the $I$ contribution is completely phenomenological. The parameters $A$ and $U$ are adjusted in order to obtain a satisfactory saturation point in the BHF approach. Together with the $V_{18}$ potential we use the values $A = -0.050$ MeV and $U = 0.00042$ MeV.

Regarding the results with the N93 interaction, some meson-exchange parameters were slightly changed with respect to those published in Ref. [14] (Table I): We now use the $(\pi, \rho)$-$N\Delta$ parameters $R_\pi = g_{\pi N\Delta}/g_{\pi NN} = 2.1$, $R_\rho = g_{\rho N\Delta}/g_{\rho NN} = 1.2$ from Ref. [25] and the $(\sigma, \omega)$-nucleon-Roper coupling constants $g^2_{\sigma NR}/4\pi = 0.7$, $g^2_{\omega NR}/4\pi = 1.4$ (and $g_{PNR} = g_{\sigma NR}$ for the Pomeron) together with the exponential $\pi NN$ form factor ($\Lambda_{\pi NN} = 1177$ MeV) in the $\pi\pi$-$NN$ contributions to the TBF. In this manner a satisfactory saturation point of nuclear matter is obtained also with this interaction.

*Results.* We now turn to the discussion of our numerical results. For practical use we provide convenient empirical parametrizations of the functional form

$$\frac{B}{A}(\rho) = \alpha\rho + \beta\rho^\gamma \tag{7}$$

for the EOS of symmetric nuclear matter and pure neutron matter obtained with the different interactions, which allow together with Eq. (5) straightforward implementation in the stellar structure equations. These simple fits reproduce the numerical data to within about 1 MeV and are certainly sufficient for the computation of stellar structure, in view of the inherent numerical and theoretical approximations of our approach.

In Table I we list the fit parameters $\alpha, \beta, \gamma$ for symmetric and neutron matter, and also show the saturation properties of nuclear matter obtained with the different interactions, namely the saturation point $[\rho, B/A]_0$, the compressibility $K = 9\rho^2\partial^2(B/A)/\partial\rho^2$, and the symmetry energy $E_{\rm sym}$ and its derivative $E'_{\rm sym} = dE_{\rm sym}/d(\rho/\rho_0)$ at normal density $\rho_0$. All interactions yield reasonable values for these physical quantities, apart from the V18 with a slightly too large saturation density and the UIX with a low compressibility. The symmetry energy derivative is in all cases compatible with the constraint 21 MeV $\lesssim E'_{\rm sym} \lesssim$ 36 MeV extracted from the analysis of isospin diffusion in heavy-ion reactions and the neutron skin of $^{208}$Pb proposed in Ref. [26]. In all cases occurs a strong displacement from the Coester band of the saturation point obtained with the two-nucleon potential alone [27].

Figure 1 shows the five TBF components, Eq. (2), obtained at normal density with the different interactions. Qualitatively one observes in all cases attractive central ($V_C$) and repulsive tensor ($V_T$) components due to the $(\pi, \rho)$-TBF, and repulsive scalar ($V_I$) parts from the $(\sigma, \omega)$-TBF [14]. The contributions

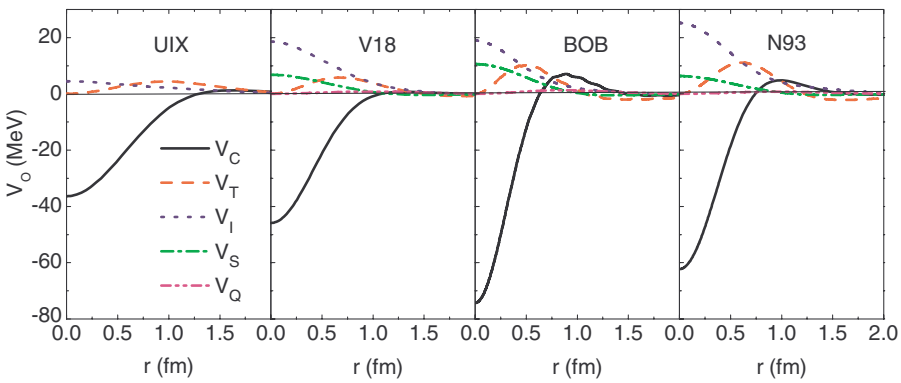


FIG. 1. (Color online) TBF components, Eq. (2), at normal density for the different interactions.

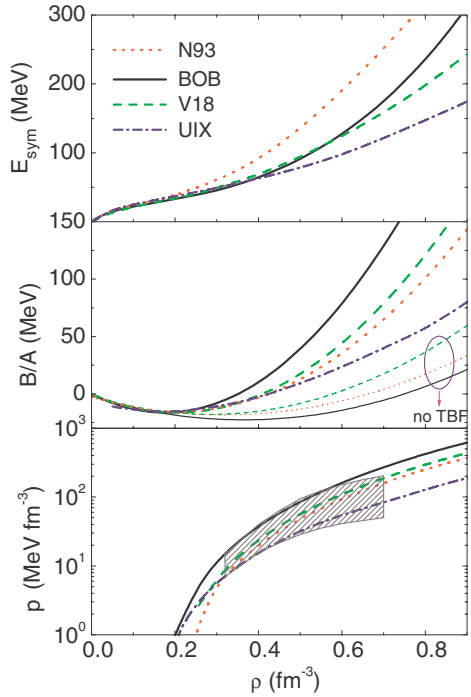


FIG. 2. (Color online) Symmetry energy (upper panel), binding energy per nucleon of symmetric nuclear matter (central panel), and pressure of symmetric matter (lower panel), employing different interactions. The shaded region indicates the constraints of Ref. [28].

$V_S$ and $V_Q$ are less important. Quantitatively the magnitudes of the different components depend strongly on the underlying meson-exchange model.

In Fig. 2 we display the symmetry energy (upper panel), the binding energy per nucleon for symmetric matter (central panel), and the pressure $p = \rho^2 \partial(B/A)/\partial\rho$ of symmetric matter (lower panel) obtained with the different interactions. While all interactions yield a satisfactory and similar behavior around normal density, there is a large and always increasing variation at high density: the UIX, N93, V18, and BOB interactions yield a more and more stiff EOS (of symmetric matter) in that order. This is due to the presence of nonlinear (in density) repulsive terms in the microscopic TBF [14], which dominate at high density. For this reason also the symmetry energies with the microscopic EOS increase stronger than linearly at large density. The pressure vs density plots fulfill the constraints due to a nuclear flow data analysis performed in Ref. [28]. Only the BOB curve exits slightly the constrained region at the largest densities.

Since presently there is no possibility of deciding which interaction is most realistic at high density, the implications of these variations for neutron star structure calculations and in particular for the maximum possible neutron star mass are certainly of interest. Figure 3 shows the mass-radius relations of nucleonic neutron stars obtained with the different interactions. As expected, the maximum mass increases with the stiffness of the EOS, ranging from about 1.8 $M_\odot$ (UIX) to 2.5 $M_\odot$ (BOB). The radii are less sensitive to the EOS and lie in the range 10–12 km for the maximum mass

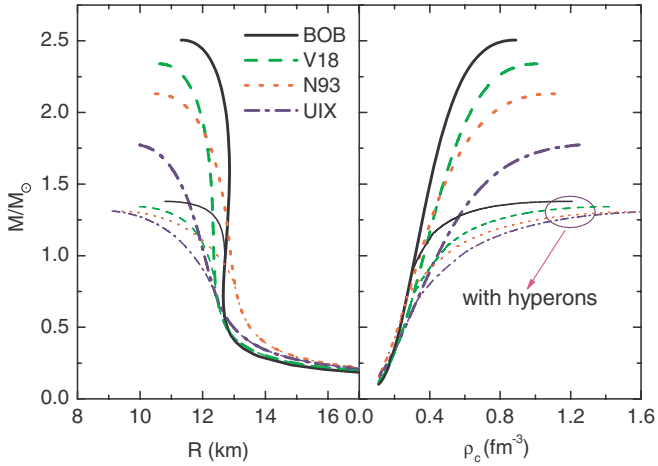


FIG. 3. (Color online) Mass-radius (left panel) and mass-central density (right panel) relations of neutron stars evaluated with different EOS.

configurations. All microscopic TBF yield substantially larger masses than the UIX, in line with the characteristics of the EOS.

We note, however, that these mass-radius relations, while mathematically correct, have to be considered unphysical due to the formation of hyperons [21,24,29–31] and/or quark matter [32] in high-density hadronic matter. For illustration we show also the effect of allowing the appearance of hyperons on the mass-radius relations (thin curves in Fig. 3). These curves have been obtained in the approximate way described in Ref. [31]: The total energy density of hypernuclear matter is split into nucleonic and hyperonic parts: $\varepsilon(\rho_N, \rho_Y) = \varepsilon_N(\rho_N) + \varepsilon_Y(\rho_N, \rho_Y)$. The nucleonic energy densities obtained in the manner described above with the different nucleon-nucleon interactions are then used together with the same hyperonic energy density function obtained with the V18+UIX nucleon-nucleon interaction and the NSC89 nucleon-hyperon forces [33], see Refs. [30,31]. Since the V18+UIX interaction is relatively soft, this procedure underestimates the importance of hyperons with the microscopic TBF and thus slightly overestimates the maximum masses in these cases.

A remarkable consequence of the inclusion of hyperons is the reduction of the large range of the maximum mass with the nucleonic EOS, 1.8–2.5 $M_\odot$, to a nearly unique value of 1.3–1.4 $M_\odot$. The hyperons (or also quark matter) provide a self-regulating softening effect on the EOS: The stiffer the original nucleonic EOS, the more it is softened by the earlier appearance and higher concentration of hyperons. In any case the maximum masses of hadronic (hyperonic) neutron stars are much too low in order to cover all present observational values. The introduction of nonhadronic "quark" matter is thus necessary [32] and heavier neutron stars can only be hybrid stars in our approach.

*Conclusions*. In conclusion, we have presented new results for the high-density nuclear EOS obtained within the BHF approach using modern two-nucleon potentials and compatible microscopic nuclear TBF. These EOS are relatively stiff and

lead to large maximum masses of purely nucleonic neutron stars, which are, however, strongly reduced by allowing the appearance of hyperons and/or quark matter.

**ACKNOWLEDGMENTS**

We would like to acknowledge valuable discussions with U. Lombardo.

[1] J. P. Jeukenne, A. Lejeune, and C. Mahaux, Phys. Rep. **25**, 83 (1976); M. Baldo, *Nuclear Methods and the Nuclear Equation of State*, International Review of Nuclear Physics, Vol. 8 (World Scientific, Singapore, 1999).

[2] R. Brockmann and R. Machleidt, Phys. Rev. C **42**, 1965 (1990); G. Q. Li, R. Machleidt, and R. Brockmann, *ibid.* **45**, 2782 (1992); P. G. Krastev and F. Sammarruca, *ibid.* **74**, 025808 (2006).

[3] D. Alonso and F. Sammarruca, Phys. Rev. C **67**, 054301 (2003).

[4] J. Carlson, V. R. Pandharipande, and R. B. Wiringa, Nucl. Phys. **A401**, 59 (1983).

[5] A. Akmal, V. R. Pandharipande, and D. G. Ravenhall, Phys. Rev. C **58**, 1804 (1998); J. Morales, V. R. Pandharipande, and D. G. Ravenhall, *ibid.* **66**, 054308 (2002).

[6] B. S. Pudliner, V. R. Pandharipande, J. Carlson, and R. B. Wiringa, Phys. Rev. Lett. **74**, 4396 (1995); Phys. Rev. C **56**, 1720 (1997).

[7] J. Carlson and R. Schiavilla, Rev. Mod. Phys. **70**, 743 (1998); R. B. Wiringa, S. C. Pieper, J. Carlson, and V. R. Pandharipande, Phys. Rev. C **62**, 014001 (2000); S. C. Pieper, K. Varga, and R. B. Wiringa, *ibid.* **66**, 044310 (2002); S. Gandolfi, F. Pederiva, S. Fantoni, and K. E. Schmidt, *ibid.* **73**, 044304 (2006); M. Pervin, S. C. Pieper, and R. B. Wiringa, *ibid.* **76**, 064319 (2007).

[8] S. C. Pieper, V. R. Pandharipande, R. B. Wiringa, and J. Carlson, Phys. Rev. C **64**, 014001 (2001).

[9] R. B. Wiringa, V. G. J. Stoks, and R. Schiavilla, Phys. Rev. C **51**, 38 (1995).

[10] R. Machleidt, K. Holinde, and Ch. Elster, Phys. Rep. **149**, 1 (1987); R. Machleidt, Adv. Nucl. Phys. **19**, 189 (1989).

[11] M. M. Nagels, T. A. Rijken, and J. J. de Swart, Phys. Rev. D **17**, 768 (1978); V. G. J. Stoks, R. A. M. Klomp, C. P. F. Terheggen, and J. J. de Swart, Phys. Rev. C **49**, 2950 (1994).

[12] P. Grangé, A. Lejeune, M. Martzolff, and J.-F. Mathiot, Phys. Rev. C **40**, 1040 (1989).

[13] W. Zuo, A. Lejeune, U. Lombardo, and J.-F. Mathiot, Nucl. Phys. **A706**, 418 (2002); Eur. Phys. J. **A14**, 469 (2002).

[14] Z. H. Li, U. Lombardo, H.-J. Schulze, and W. Zuo, Phys. Rev. C **77**, 034316 (2008).

[15] B. D. Day, Phys. Rev. C **24**, 1203 (1981); H. Q. Song, M. Baldo, G. Giansiracusa, and U. Lombardo, Phys. Rev. Lett. **81**, 1584 (1998); M. Baldo, G. Giansiracusa, U. Lombardo, and H. Q. Song, Phys. Lett. **B473**, 1 (2000); M. Baldo, A. Fiasconaro, H. Q. Song, G. Giansiracusa, and U. Lombardo, Phys. Rev. C **65**, 017303 (2001); R. Sartor, *ibid.* **73**, 034307 (2006).

[16] X. R. Zhou, G. F. Burgio, U. Lombardo, H.-J. Schulze, and W. Zuo, Phys. Rev. C **69**, 018801 (2004).

[17] B. H. J. McKellar and R. Rajaraman, Phys. Rev. C **3**, 1877 (1971); D. W. E. Blatt and B. H. J. McKellar, *ibid.* **11**, 614 (1975).

[18] S. A. Coon, M. D. Scadron, P. C. McNamee, B. R. Barrett, D. W. E. Blatt, and B. H. J. McKellar, Nucl. Phys. **A317**, 242 (1979).

[19] M. Baldo and L. S. Ferreira, Phys. Rev. C **59**, 682 (1999).

[20] I. Bombaci and U. Lombardo, Phys. Rev. C **44**, 1892 (1991); L. Engvik, M. Hjorth-Jensen, E. Osnes, G. Bao, and E. Ostgaard, Astrophys. J. **469**, 794 (1996).

[21] M. Baldo, G. F. Burgio, and H.-J. Schulze, Phys. Rev. C **58**, 3688 (1998).

[22] W. Zuo, I. Bombaci, and U. Lombardo, Phys. Rev. C **60**, 024605 (1999); E. N. E. van Dalen, C. Fuchs, and A. Faessler, *ibid.* **72**, 065803 (2005).

[23] M. Baldo, I. Bombaci, and G. F. Burgio, Astron. Astrophys. **328**, 274 (1997).

[24] N. K. Glendenning, *Compact Stars: Nuclear Physics, Particle Physics and General Relativity*, 2nd ed. (Springer, Berlin, 2000).

[25] Th. A. Rijken and V. G. J. Stoks, Phys. Rev. C **46**, 73 (1992); **46**, 102 (1992).

[26] Bao-An Li and A. W. Steiner, Phys. Lett. **B642**, 436 (2006).

[27] Z. H. Li, U. Lombardo, H.-J. Schulze, W. Zuo, L. W. Chen, and H. R. Ma, Phys. Rev. C **74**, 047304 (2006).

[28] P. Danielewicz, R. Lacey, and W. G. Lynch, Science **298**, 1592 (2002).

[29] H. Heiselberg and M. Hjorth-Jensen, Phys. Rep. **328**, 237 (2000).

[30] M. Baldo, G. F. Burgio, and H.-J. Schulze, Phys. Rev. C **61**, 055801 (2000).

[31] H.-J. Schulze, A. Polls, A. Ramos, and I. Vidaña, Phys. Rev. C **73**, 058801 (2006).

[32] G. F. Burgio, M. Baldo, P. K. Sahu, and H.-J. Schulze, Phys. Rev. C **66**, 025802 (2002); M. Baldo, M. Buballa, G. F. Burgio, F. Neumann, M. Oertel, and H.-J. Schulze, Phys. Lett. **B562**, 153 (2003); C. Maieron, M. Baldo, G. F. Burgio, and H.-J. Schulze, Phys. Rev. D **70**, 043010 (2004); M. Baldo, G. F. Burgio, P. Castorina, S. Plumari, and D. Zappalà, Phys. Rev. C **75**, 035804 (2007); T. Maruyama, S. Chiba, H.-J. Schulze, and T. Tatsumi, Phys. Rev. D **76**, 123015 (2007).

[33] P. M. M. Maessen, Th. A. Rijken, and J. J. de Swart, Phys. Rev. C **40**, 2226 (1989).